



## Temporal constraints on fracturing associated with fault-related folding at Sant Corneli anticline, Spanish Pyrenees

J. Ryan Shackleton<sup>a,\*</sup>, Michele L. Cooke<sup>a</sup>, Jaume Vergés<sup>b</sup>, Toni Simó<sup>c</sup>

<sup>a</sup> University of Massachusetts, Amherst, 611 North Pleasant Street, Amherst, MA 01003-9297, United States

<sup>b</sup> Institute of Earth Sciences "Jaume Almera", CSIC, Lluís Solé i Sabarís s/n, 08028 Barcelona, Spain

<sup>c</sup> ExxonMobil, URC, 3120 Buffalo Speedway, Houston, TX 77098, United States

### ARTICLE INFO

#### Article history:

Received 12 February 2009

Received in revised form

27 October 2010

Accepted 2 November 2010

Available online 13 November 2010

#### Keywords:

Sant Corneli

St Corneli

Fractures

Joints

Folding

Growth strata

Syn-tectonic

### ABSTRACT

We mapped fractures at Sant Corneli anticline, an E–W trending non-cylindrical, fault-related anticline in the Spanish Pyrenees. Fracture mapping in syn-tectonic strata directly links fold-related fracturing to fold evolution because the relationship of fractures to syn-tectonic strata can constrain structural timing. Rather than using absolute fracture orientation as a primary means of grouping fracture sets, we used relative fracture timing, mineral fill, fracture size (length and height), and orientation with respect to bed strike to delineate five bed-orthogonal fracture sets that we interpret to be associated with folding and faulting events. We observe several early sets of joints with calcite fill (J1, J2, J3) many of which are interpreted to be related to fold axis perpendicular normal faulting of the anticline. Two late-stage joint sets with associated iron oxide mineralization in the surrounding wall rock (J4, J5) are oblique to bedding, maintain orientation with respect to bed strike, and are interpreted to result from flexure of the anticline. We infer the timing of J4/J5 jointing relative to syn-tectonic events. This research demonstrates how fracture studies that integrate syn-tectonic strata and distinguish fracture sets on the basis of multiple characteristics can better constrain the timing of fracturing relative to regional deformation events.

© 2010 Elsevier Ltd. All rights reserved.

### 1. Introduction

The ability to quantitatively predict the orientation and density of natural fractures is advantageous in many industries because subsurface fracture networks form fluid flow pathways and reservoirs in groundwater aquifers, hydrocarbon reservoirs, and hydrothermally active basins. Fracture prediction in layered sedimentary rocks relies heavily on layer shape (fold shape) and fault shape. Fold shape affects fracturing because bending stresses control the density and orientation of fractures in three dimensions (Szilard, 1974; Fischer and Wilkerson, 2000). Faults exert a significant control on both the overall fold shape and the stress field near fault tips (e.g. Pavlis and Bruhn, 1988; McGrath and Davison, 1995; Rudnicki and Wu, 1995; Savage and Cooke, 2004; Bellahsen et al., 2006). Field studies of fracturing in fault-related folds serve two roles in fracture prediction. First, natural structures can be used to test theoretical predictions for fracturing based on plate bending, faulting, or other models for fracture formation (e.g. Hennings et al., 2000; Bergbauer and Pollard, 2004; Bellahsen et al., 2006). Second, field studies can inform subsurface predictions of fracture

networks, which are commonly below the resolution of many geophysical techniques.

Inferring the fracture history and geometry in a fault-related fold requires an understanding of the evolution of the fold shape through time. Geologists have devised a number of approaches to understanding such folds, including forward geometric and geo-mechanical fold modeling (e.g. Suppe, 1983; Suppe and Medwedeff, 1990; Erslev, 1991; Poblet and McClay, 1996; Johnson and Johnson, 2002), structural restoration algorithms (Rouby et al., 2000; Griffiths et al., 2002; Thibert et al., 2005; Maerten and Maerten, 2006), and studies of natural folds and numerically modeled folds with syn-tectonic strata (Vergés et al., 1996; Ford et al., 1997; Poblet et al., 1998; Novoa et al., 2000; Salvini and Storti, 2002a). Natural folds with syn-tectonic strata provide direct evidence of changes in fold shape because each syn-tectonic horizon can be individually restored to document fold shape at a particular time (e.g. Vergés et al., 1996; Ford et al., 1997; Poblet et al., 1998; Novoa et al., 2000; Bernal and Hardy, 2002; Salvini and Storti, 2002b). While syn-tectonic strata have been used extensively to understand fold evolution, relatively few studies have utilized syn-tectonic strata to understand the evolution of fracturing and small scale structures associated with folding (e.g. Nigro and Renda, 2004), which is the purpose of this study.

\* Corresponding author.

E-mail address: [ryan@geo.umass.edu](mailto:ryan@geo.umass.edu) (J.R. Shackleton).

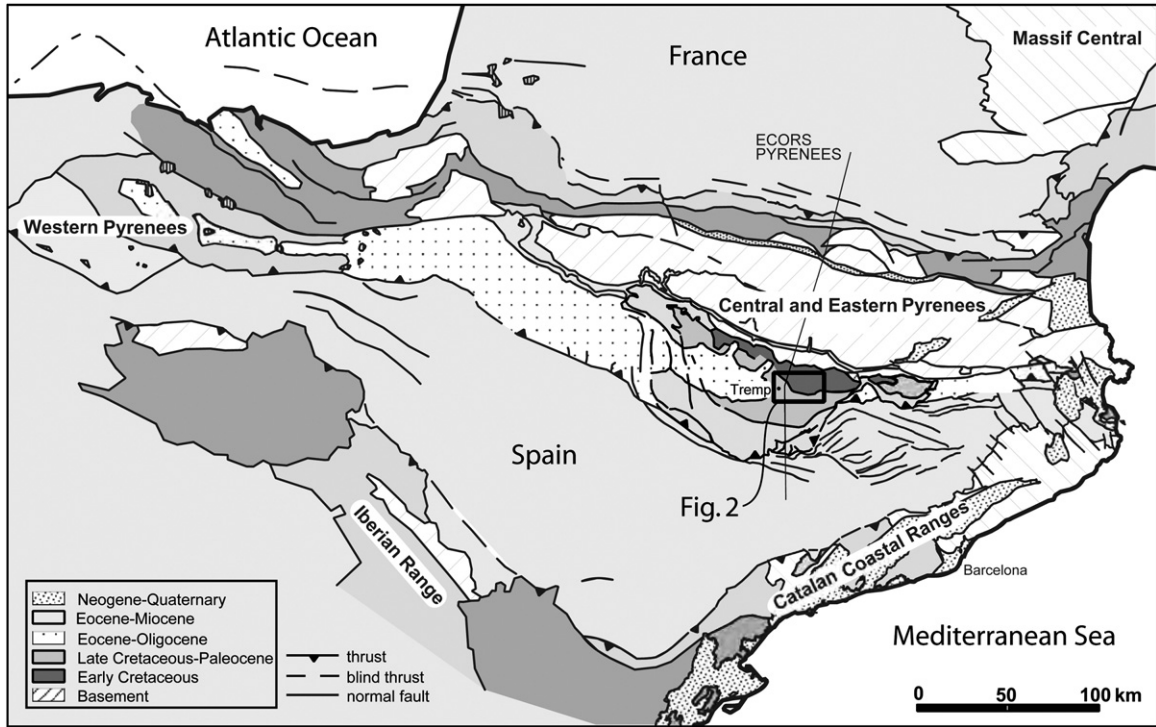


Fig. 1. Generalized map of the Spanish Pyrenees showing the major thrusts. The Southern Central Unit, a thrust-bounded block containing the Boixols thrust and Sant Corneli Anticline, is highlighted in the center of the map. (modified from Vergés, 1993)

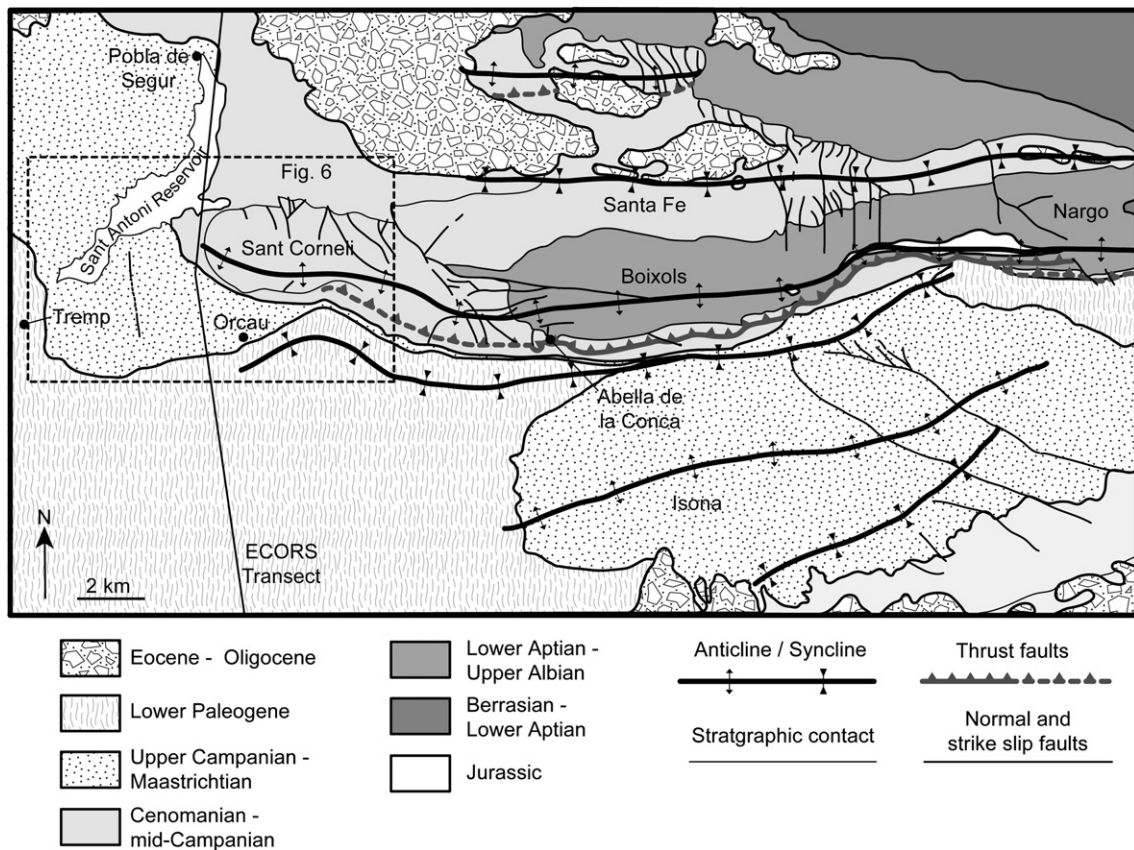


Fig. 2. Geologic map of the Sant Corneli-Boixols-Nargo anticline. Thrusts shown at the surface south of the Sant Corneli and Boixols anticlines are relatively small displacement thrusts that splay off of the Boixols thrust. The dotted box indicates the boundaries of the study area and the location of Fig. 5. (modified from Bond and McClay, 1995).

Field studies of fractures associated with fault-related folding have suffered from a crucial lack of data linking the changes in fold shape through time to specific fracturing events. Early conceptual models for fold-related fracturing (Stearns, 1967; Stearns and Friedman, 1972) have been criticized because their predictions are based entirely on the final fold shape, neglecting transitional fold shapes, pre-existing fracture patterns, and stresses associated with an underlying fault tip (McGrath and Davison, 1995; Fischer and Wilkerson, 2000; Bergbauer and Pollard, 2004; Savage and Cooke, 2004; Bellahsen et al., 2006). More recent studies have focused on distinguishing fold-related fractures from pre- and post-fold fractures, however, fold-related fractures are usually grouped into “early folding” or “late folding” episodes with little direct evidence for fracture timing relative to specific folding events (e.g. Cooper, 1992; Engelder et al., 1997; Hanks et al., 1997; Hennings et al., 2000; Shackleton, 2003; Bergbauer and Pollard, 2004; Bellahsen, 2006). The disconnect between evidence for fracture evolution and fold evolution largely stems from the fact that cross-cutting relationships between fractures only reflect the *relative* timing of fracturing events without the context of fold evolution.

The Sant Corneli anticline is a plunging thrust-related anticline in the Spanish Pyrenees that offers the opportunity to document the history of fracturing in the context of a well constrained fold history (Figs. 1, 2 and 3). The anticline is well exposed in three dimensions and has excellent exposures that are well suited to field mapping of fractures (Fig. 4). Additionally, the geometry of adjacent syn-tectonic strata constrains aspects of the fold evolution such as limb rotation and lateral fold propagation (e.g. Vergés et al., 1996; Ford et al., 1997; Novoa et al., 2000; Bernal and Hardy, 2002; Maerten and Maerten, 2006; Guillaume et al., 2008). Further, fracture mineralization links fractures to specific depositional and structural events during folding, thus directly linking fold evolution to the observed fracture sequence. We use the syn-tectonic framework to create a template of the relationships between fractures and the host fault-related anticline for future structural modeling studies.

## 2. Tectono-stratigraphic evolution of the Sant Corneli anticline

The Sant Corneli anticline, situated in the southern central Pyrenees of Spain (Fig. 1), formed during the Late Cretaceous and Eocene–Oligocene periods in response to the collision of Iberia with Europe (Puigdefàbregas and Souquet, 1986; Roest and Srivastava, 1991). Sant Corneli anticline is an asymmetric, westerly plunging anticline that forms the termination of the Bóixols thrust, a nearly 40 km long, east–west trending, south-vergent thrust (Berástegui et al., 1990; Puigdefàbregas et al., 1992; Bond and McClay, 1995; García-Senz, 2002). The Sant Corneli–Bóixols–Nargó anticlines formed above detachments in Triassic evaporates (Fig. 3), as a result of inversion of the lower Cretaceous Organyà extensional basin (Berástegui et al., 1990; Déramond et al., 1993; Vergés, 1993; Bond and McClay, 1995). Evidence for the structural history of the Sant Corneli–Bóixols–Nargó anticlines is contained in the sedimentary record of the late Cretaceous–Oligocene strata that overlie the anticline.

### 2.1. Stratigraphic history

At the first-order, the Sant Corneli anticline exposes a core of intensely fractured and faulted carbonate rocks capped by gray marls overlain by a sequence of syn-tectonic marls and sandstones (Figs. 3 and 4, Garrido-Megías and Ríos Aragües, 1972). The anticlinal core is primarily composed of Triassic to mid-Cretaceous terrestrial and carbonate rocks of the Organyà basin (Simó et al., 1985; Simó 1989). The overlying Sant Corneli sequence consists of

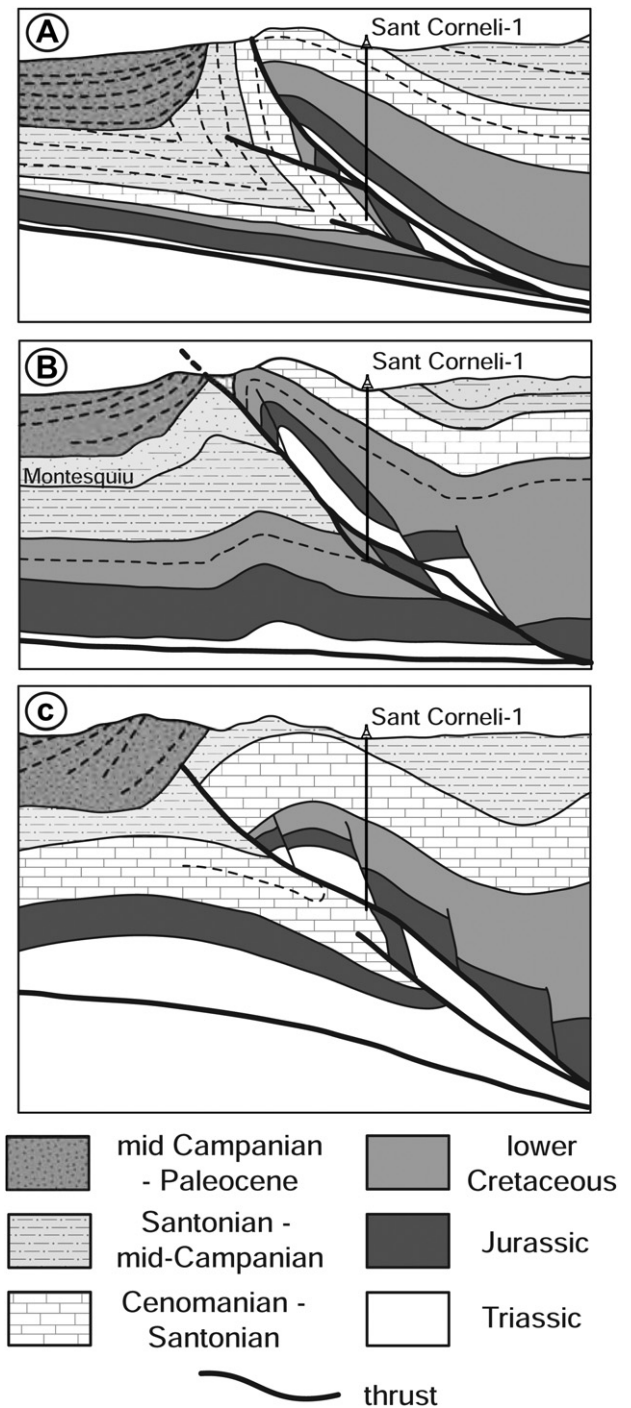


Fig. 3. Cross sections through Sant Corneli anticline along or near the ECORS transect (Fig. 2). A) Déramond et al. (1993), B) Vergés (1993), and C) García-Senz (2002).

platform carbonates and calc-arenites representing the edge of a basin that deepened to the northwest during the Coniacian–Santonian (late Cretaceous, Simó et al., 1985; Simó, 1985; Puigdefàbregas and Souquet, 1986; Simó, 1989). A regional angular unconformity separates the Sant Corneli sequence from the overlying Vallcarga sequence, which in the study area consists primarily of turbiditic marls, limestones, and clays (Nagtegaal et al., 1983; Ardévol et al., 2000). Paleocurrents and dramatic thickening of the Vallcarga sequence to the northwest of the Sant Corneli anticline indicate that the area was paleo-high during Campanian time, although it is unclear whether the Sant Corneli anticline was

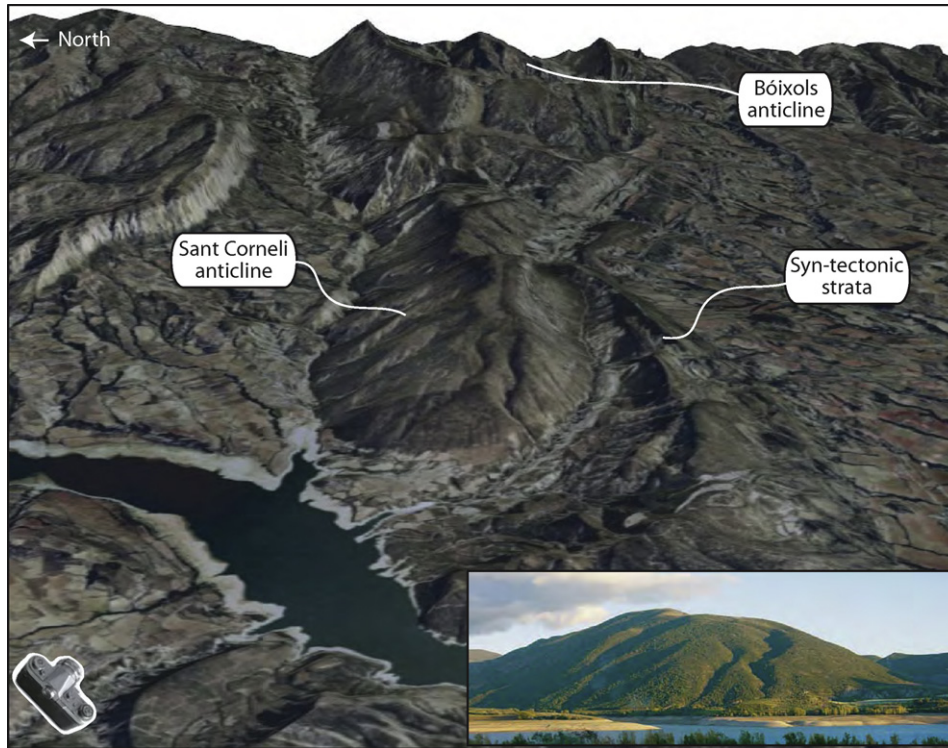


Fig. 4. Digital elevation model with orthophoto drape of Sant Corneli anticline. View is east. The topographic expression of Sant Corneli mountain roughly corresponds to the shape of the Sant Corneli sequence. Camera image (bottom right) shows the viewing direction of the inset photo, which shows the shape of the backlimb and fold nose.

tectonically active during deposition of the marls (Van Hoorn, 1970; Garrido-Megías and Ríos Aragües, 1972; Nagtegaal et al., 1983; Ardévol et al., 2000).

Though the Aren group has been subdivided differently by different authors (Garrido-Megías and Ríos Aragües, 1972; Nagtegaal et al., 1983; Simó et al., 1985; Simó 1989; Puigdefàbregas and Souquet, 1986; Specht et al., 1991; Déramond et al., 1993; Arbués et al., 1996; Ardévol et al., 2000), this paper will use the naming conventions delineated by Déramond et al. (1993) and revised by Guillaume et al. (2008). Growth faulting and olistoliths mark the base of the syn-tectonic Aren Group (Montesquiu sequence). The Puimanyons olistostrome is interpreted to represent basin margin collapse, possibly resulting from the initial Boixols thrusting and amplification of Sant Corneli anticline (Fig. 5A, Simó, 1985). The overlying Salas Marls represent the deeper basinal rocks of a northwestward-prograding sequence of nearshore to offshore siliciclastic rocks (Fig. 5B, Nagtegaal et al., 1983; Simó et al., 1985; Simó 1989; Déramond et al., 1993). The Montesquiu sequence is cut deeply at Sant Corneli by a karst surface with locally incised valleys indicating subaerial erosion and sedimentary transport toward the northwest (Fig. 5B, Nagtegaal et al., 1983; Simó et al., 1985; Simó 1989; Ardévol et al., 2000). The Orcau-Vell sequence overlies the karst surface and consists of fluvial channel fill to the east and tide-influenced bioclastic bars in a rapidly deepening basin to the west (Déramond et al., 1993; Guillaume et al., 2008).

An erosional surface forms the base of the Santa Engracia sequence, which consists of significantly more terrigenous and coarser facies than the underlying Orcau-Vell sequence (Simó et al., 1985; Simó 1989; Guillaume et al., 2008). Part of the basal surface of the Santa Engracia sequence is interpreted to be formed by a north-northwest oriented, gravity driven fault based on the interruption of the underlying systems tracts in the Orcau-Vell sequence (Figs. 6 and 7D). Déramond et al. (1993) and Guillaume et al. (2008) suggest that the fault created significant accommodation space for channelized,

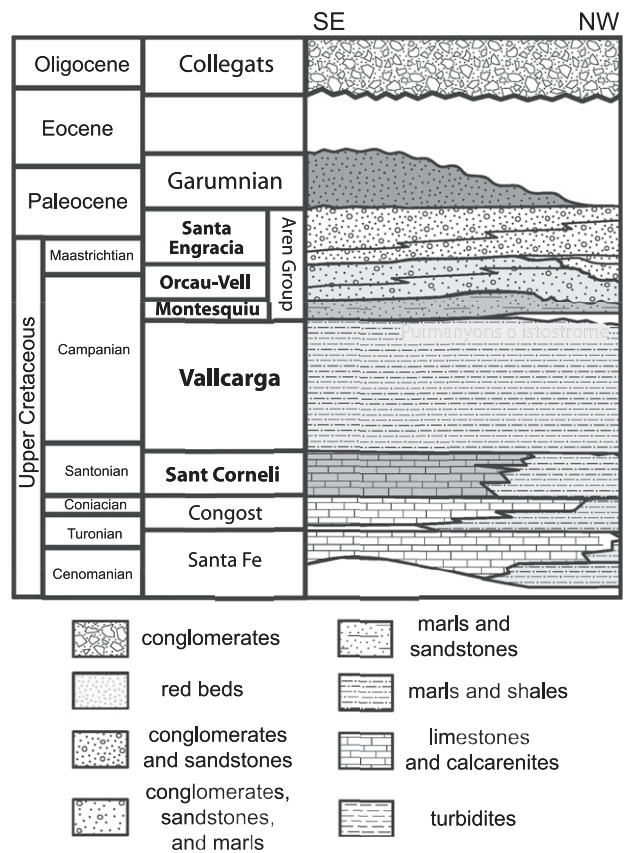
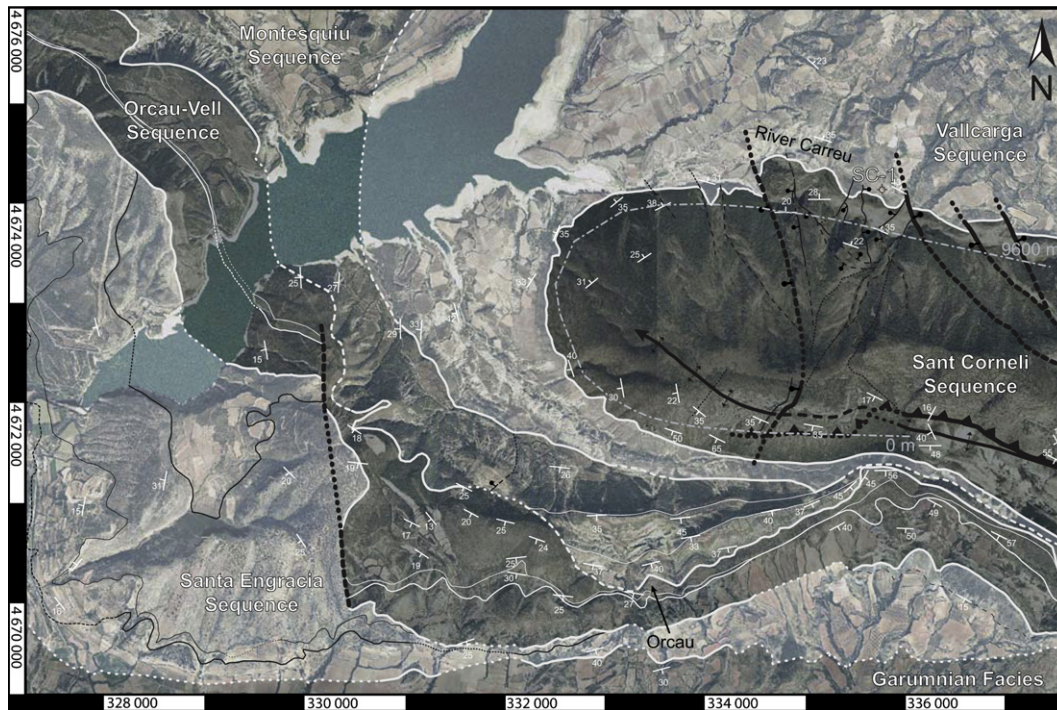


Fig. 5. Simplified stratigraphic section showing the major stratigraphic sequences. Names in bold represent sequences referred to in the text and shown on Fig. 6, other names (non-bold) refer to formation or facies names unless otherwise specified. (modified from Déramond et al., 1993; Bond and McClay, 1995 and Ardévol et al., 2000).



**Fig. 6.** Geologic map of the study area showing the major structural elements and stratigraphic sequences. Solid lines are exposed contacts, dashed lines are covered or poorly exposed contacts, and dotted lines are inferred contacts. SC-1 indicates the location of the Sant Corneli-1 well. Dash-dotted line indicates the location of the traverse in Fig. 18 (Orcau-Vell and Santa Engracia contacts modified from Guillaume et al., 2008).

quartz rich slope fan and Gilbert-type deltaic deposits with transport directions toward the southwest (Simó et al., 1985; Déramond et al., 1993; Guillaume et al., 2008). The upper surface of the slope fan and deltaic deposits is oxidized and represents significant base level fall and subaerial erosion (Guillaume et al., 2008).

The upper Santa Engracia sequence consists of a carbonate marine transgressive systems tract overlain by a deltaic highstand systems tract indicating base level rise after subaerial erosion (Déramond et al., 1993; Guillaume et al., 2008). Terrestrial fluvial deposits of the Garumnian facies overlie the Santa Engracia sequence and were deposited during the growth of the Sant Corneli and Boixols structures as observed to the east of the study area (Garrido-Megías and Ríos Aragües, 1972). The Garumnian facies are interpreted to have been deposited during a period of relative tectonic quiescence in the southern Pyrenees (Nagtegaal et al., 1983; Simó et al., 1985; Déramond et al., 1993; Bond and McClay, 1995; Guillaume et al., 2008). Subsequent amplification of the Sant Corneli anticline occurred during the deposition of the upper part of the La Pobla conglomerates that show growth geometry against the northern flank of the fold (Puigdefàbregas et al., 1992; Mellere, 1993).

## 2.2. Fold/thrust structure of Sant Corneli anticline

The major geomorphic expression of Sant Corneli anticline is defined by the Sant Corneli sequence, which is folded into an asymmetric, open anticline at the surface with a steep westward plunge of approximately 25°. While the backlimb is relatively planar, the transition on the fold nose from ~25° north dipping beds in the backlimb to ~50° south dipping beds in the forelimb occurs without significant kinking or faulting as evidenced by the continuous outcrop trace of the contact of the Sant Corneli sequence with the overlying marls (Figs. 4 and 6). In contrast, the transition from nearly horizontal dipping beds on the crest of the anticline to steeper dipping beds on the forelimb is abrupt in the core of the anticline (Fig. 6).

The subsurface structure of Sant Corneli anticline is mostly constrained by one ~3000 m deep well in the backlimb of the anticline (SC-1, Figs. 3 and 6). The Sant Corneli-1 well penetrates an upright sequence of Triassic, Jurassic, and Cretaceous rocks overlying a fault, below which is an inverted and condensed Jurassic and Cretaceous sequence (Lanaja et al., 1987). The missing strata across the fault suggests between 2650 and 3580 m of displacement at Sant Corneli anticline depending on the subsurface fault configuration (García-Senz, 2002), although no evidence for large displacement faults is observed at the surface. One interpretation for the apparent discrepancy in displacement is that the main Bóixols thrust breached the surface and was eroded by one or more of the intra-Campanian or Maastrichtian unconformities (Garrido-Megías and Ríos Aragües, 1972; Berástegui et al., 1990; García-Senz, 2002). According to this interpretation, the Bóixols thrust continues beneath Sant Corneli anticline and is buried by the Aren group somewhere beneath the village of Orcau (Figs. 2 and 6).

## 2.3. Timing of fold amplification from growth strata

The Aren group is only present in the forelimb and on the fold nose, where progressive folding during deposition is indicated both by changes in sedimentary facies and sediment transport direction, as well as by progressive unconformities (Figs. 2, 5 and 6). The Aren group thins dramatically to the east, where it lies unconformably on Santonian and older carbonate units showing the overall westward direction of lateral growth. In the forelimb east of Orcau (Fig. 6), the Sant Corneli sequence dips approximately ~5–10° steeper than the overlying Montesquiu/Orcau-Vell sequence, which indicates relatively low structural relief of Sant Corneli anticline during deposition of the Montesquiu sequence (Figs. 6 and 7C). The next significant discrepancy in dip (~15°) within the Aren group is across the unconformity at the base of the Orcau-Vell sequence near Orcau. The dip discrepancy between the Orcau-Vell and the Santa Engracia sequences in the forelimb of the anticline is up to 35° in

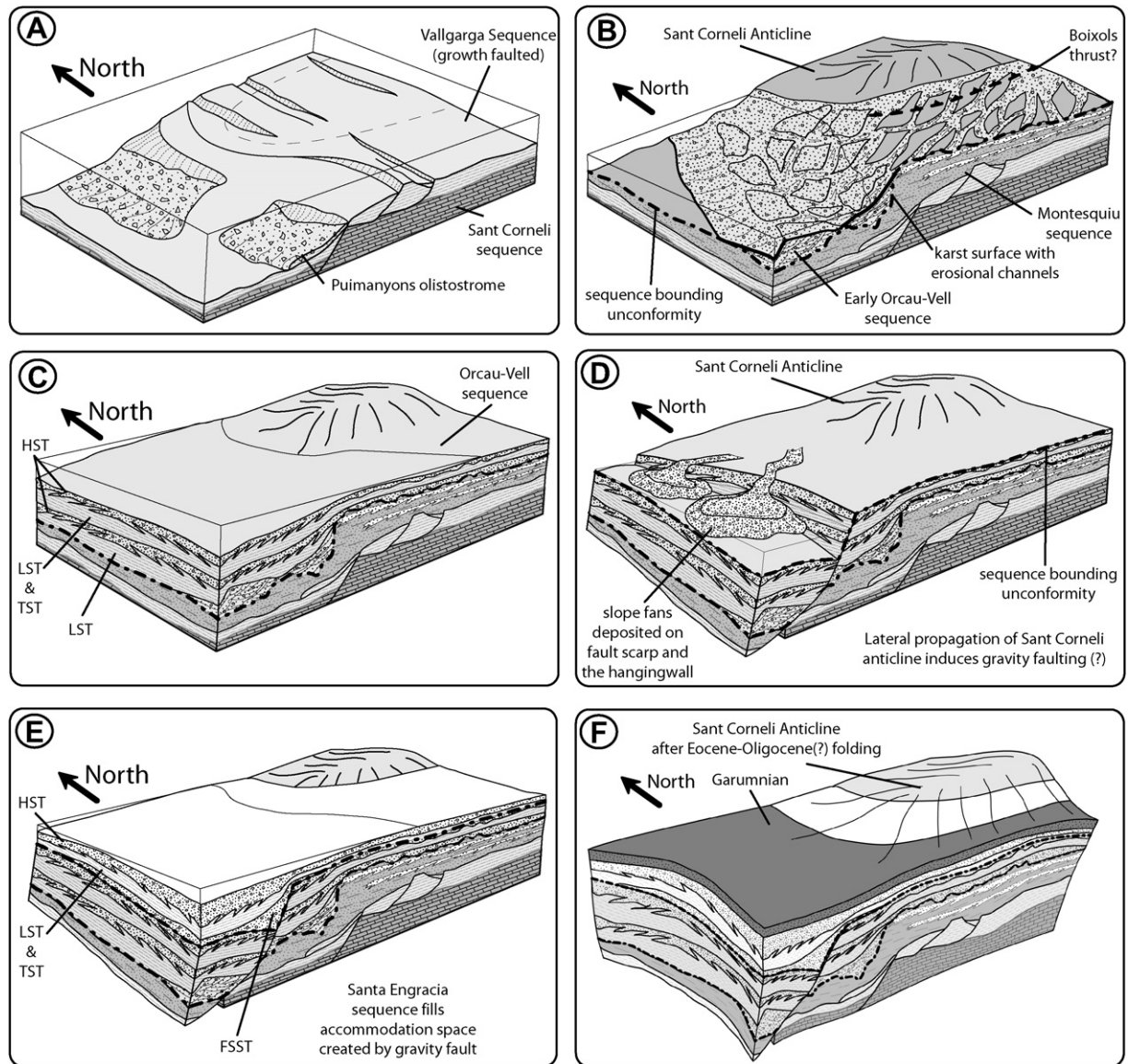


**Fig. 7.** Simplified paleogeography and structural evolution of the study area. A) earliest Montesquiu time, B) earliest Orcau-Vell time, C) end of Orcau-Vell time, D) earliest Santa Engracia time, E) end of Santa Engracia time, F) after (Eocene–Oligocene) folding of the Santa Engracia and Garumnian sequences. HST: highstand systems tract, LST: lowstand systems tract, TST: transgressive systems tract, FSST: falling stage systems tract.

the eastern end of the study area, indicating significant folding and tilting of the strata east of Orcau during deposition of the Santa Engracia sequence.

The present limb dips of the Aren group at Sant Corneli anticline ( $15\text{--}50^\circ$ ), as well as tilting of the overlying Garumnian rocks indicate that further folding and limb rotation occurred after deposition of the Aren group and the overlying Garumnian terrestrial deposits (Fig. 7F). This additional amplification predates deposition of the Eocene–Oligocene (Collegats) conglomerates (Figs. 2 and 5), which dip shallowly north, and unconformably overlie the Vallgarga sequence north of the study area (Fig. 5).

### 3. Field mapping of faults and fractures at Sant Corneli anticline

#### 3.1. Fracture mapping methodology

Our field mapping of fractures (joints and faults) in the Aren and Sant Corneli sequences constrains the stress-strain history of the

anticline. Fracture mapping of pavement outcrops facilitates documentation of the relative timing between fracture sets. Pavement outcrops of sandy lithologies in the Aren group provide the most robust timing relationships due to the size and quality of outcrop. In contrast, pavement outcrops in the less resistant Sant Corneli Sequence are generally smaller with fewer cross-cutting relationships preserved. Data collected at each site includes the orientation, mode of deformation, length (parallel to bedding), height (perpendicular to bedding), presence or absence of fracture fill, fracture fill type, and terminations or cross-cutting relationships. Because the focus of this study is to document the timing relationships between fracture sets and the fracture history of the anticline, fracture intensity data were not extensively collected.

Because bed strike changes rapidly in the Sant Corneli anticline (Fig. 6), absolute fracture orientation, or even fracture orientation after unfolding is not the sole criterion for defining fracture sets. We distinguished fracture sets using fracture orientation with respect to bed strike, fracture fill type or absence of fill, fracture size (length and height), and timing relationships with respect to other

fractures (e.g. Grout and Verbeek, 1998). Using this range of criteria, we did determine that grouping fracture types by their orientation with respect to the present-day bedding strike is a valid first approximation.

In the following description and discussion, the term “joint” refers to fractures with evidence of opening during formation, such as sparry or euhedral calcite fill, joint surface textures, planar and through-going fracture faces, and systematic fracture spacing (Pollard and Aydin, 1988). We use the term “fault” where fractures clearly initiated in shear and the term “fracture” where the mode of formation is unclear. Approximately 10 percent of the fractures we documented are not included in any fracture set because such fractures may be similarly oriented to fractures of a nearby set, but differ in length, height, fill type, or deformation mode (opening vs. shear).

### 3.2. Joint and fault sets

#### 3.2.1. NNE to NNW striking normal faults

NNE to NNW striking normal faults are the most predominant second-order structures between the fold nose and the cylindrical part of the anticline to the east (Figs. 6 and 8). Faults in the backlimb strike NNW, while normal faults in the forelimb strike NNE (Fig. 6). Normal faults are best exposed in the backlimb of the anticline in the Sant Corneli sequence, although normal faults are present in the Sant Corneli sequence in the forelimb, as well as in the Vallcarga and Montesquiu sequences in the forelimb, nose and backlimb (Fig. 8A). The largest NNW striking fault in the backlimb offsets the top of the Sant Corneli sequence by approximately 100 m with displacement down to the west (Fig. 6). Abundant smaller faults with meter and sub-meter scale offsets have  $\sim 70^\circ$  dips and similar strike to the larger fault (Fig. 8B). Many faults are mineralized with sparry calcite fill and matrix-supported fault breccias that thicken to cm scale where fault asperities create openings along the fault plane. In general, NNW and NNE striking normal faults in the Sant Corneli sequence contain only sparry calcite, with the exception of one well-exposed, low-angle (NW striking,  $\sim 45^\circ$  W dipping) normal fault east of the Sant Corneli-1 well (Fig. 6); this fault contains a 0.5 m zone of brecciated wall-rock fragments in a matrix of sparry calcite and hematite.

Low-angle normal faults are present in the overlying Vallcarga and Aren marl units (Fig. 8A). These faults commonly have thin (1–3 cm) calcite fill, exhibiting multiple generations of slickensides that indicate predominantly normal displacement. Almost all have a  $\sim 5$  cm oxidation halo of iron and goethite mineralization of the wall rock surrounding the faults (Fig. 8A). Most faults in their restored state strike N–S, dip east, and appear to sole into shallow detachments above the top of the Sant Corneli sequence. Displacement on faults in the Vallcarga increases to the west, in some cases forming large blocks with growth stratigraphy.

NNW striking,  $\sim 50^\circ$  W dipping normal faults are also present in the Aren group, the most important example is an inferred growth fault with approximately 150 m of displacement in the upper Aren group (indicated by the dotted fault near the words “Santa Engracia Sequence” in Fig. 6, and shown schematically in Fig. 7D) (Specht et al., 1991; Déramond et al., 1993; Guillaume et al., 2008).

#### 3.2.2. WNW striking normal faults

Three map-scale WNW striking normal faults are present in the backlimb near the River Carreu. Two faults that cross the River Carreu near the northeastern end of the study area dip north, whereas one fault between the north dipping faults dips south (Fig. 6). Smaller faults of the same orientation are filled with calcite and hematite cements with slickensurfaces indicating normal displacement. The displacement of WNW striking faults appears to be significantly less than that of the NNW/NNE striking faults.

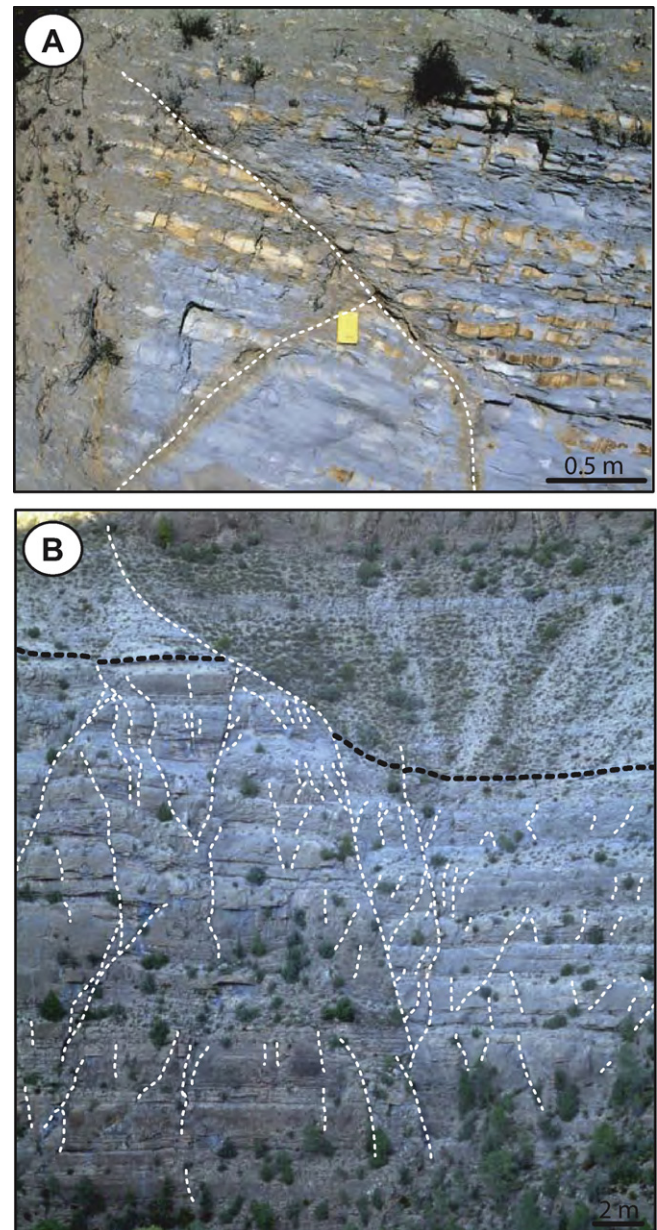


**Fig. 8.** Photos of normal faults in the field area. A) View south at a typical N–S striking low-angle fault in the Vallcarga sequence (backlimb). B) View south of NW-striking faults (dotted white lines) in the backlimb of Sant Corneli anticline. An offset marker horizon at the base of an interbedded calc-arenite/marl unit is shown in black.

#### 3.2.3. NNW striking calcite-filled joints (J2)

NNW striking calcite-filled joints in the Aren group are generally 0.5–3 m in length and are planar and very systematic with spacing on the order of a meter to a few meters (Fig. 9). These joints are locally echelon and commonly have large apertures up to 4 mm that are healed by sparry and locally fibrous calcite cement (Fig. 10A and B). Where observable, the spacing of NNW filled joints scales to the thickness of the shoreface and shallow marine sandstone lithologies in the Montesquiu and Orcau-Vell sequences, which tend to be 1–5 m (Ardévol et al., 2000). NNW striking joints maintain a consistent orientation for at least a few kilometers on either side of Orcau, but are not observed in the underlying Sant Corneli sequence (Fig. 11).

#### 3.2.4. Calcite-filled joints at large angles to bed strike (J1/J3)

In the Aren group, NNE striking calcite-filled joints (Fig. 12) range in length from a few centimeters to 2 m in length with

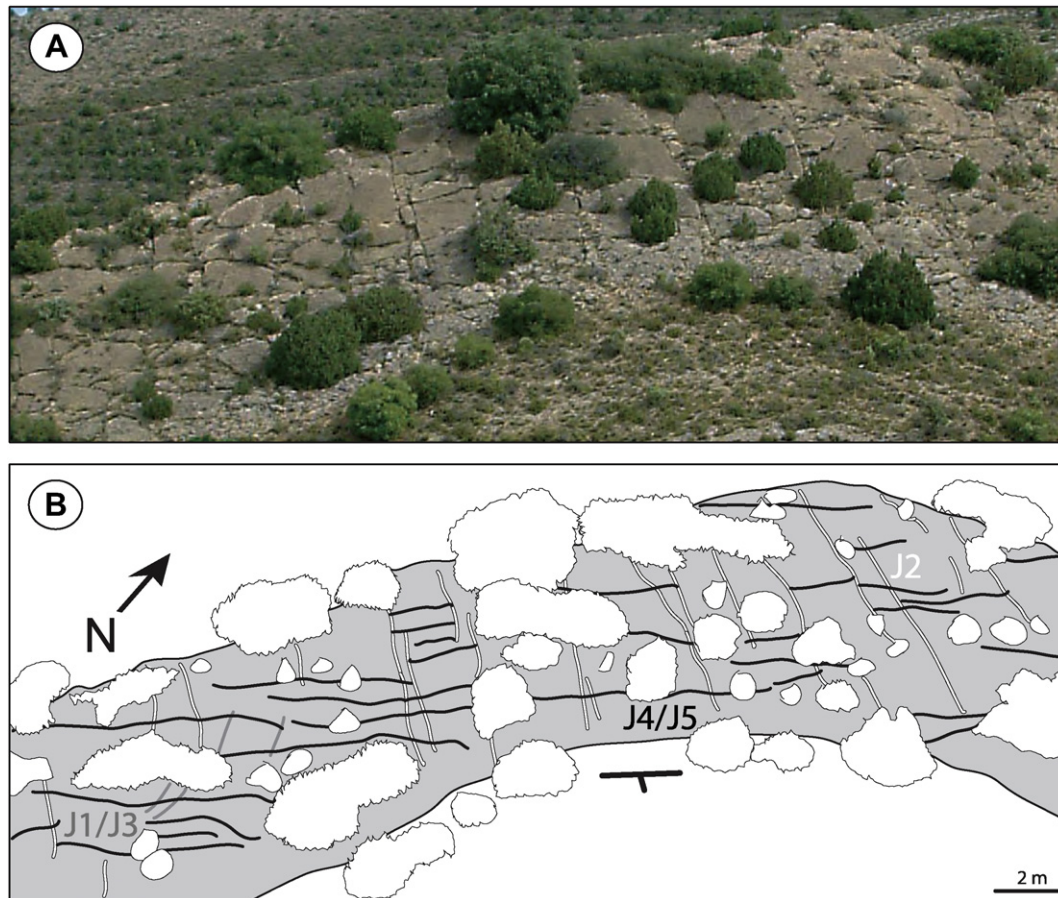


Fig. 9. View northwest at a pavement outcrop in the Montesquiu sequence near Orcau. A) image, B) interpretive sketch.

apertures up to 4 mm (Fig. 10C and D). Cross-cutting calcite fill of the different healed joint sets provides definitive evidence of joint relationships, but the relative timing of this set is complicated by conflicting cross-cutting relationships. Though the orientation, size, and fill of NNE striking joints is indistinguishable to the naked eye, some NNE striking joints are crosscut by (Fig. 10C and D), and therefore pre-date, NNW striking calcite-filled joints (J2), whereas other NNE striking joints crosscut and/or are associated with the NNW striking (J2) set. Further evidence for late NNE striking (J3) jointing in the Aren group includes NNE striking joint splays off of NNW striking (J2) joints and swarms of NNE striking joints near some NNW striking (J2) joints. Thus, the J1/J3 joint set consists of at least two subsets, one (J1) that pre-dates the J2 joints, and one (J3) that post-dates the J2 joints. Because we cannot distinguish these subsets except where age relationships to J2 joints are preserved, we refer to this set as J1/J3.

In the Sant Corneli sequence, NNW striking (backlimb) and NNE striking (forelimb) calcite-filled joints are nearly perpendicular to bed strike and are present at a variety of sizes, from cm to meter scale. These joints usually have 1–4 mm of sparry calcite fill, with sharp, planar contacts with the surrounding wall rock (Fig. 14). Joints of this set have similar strike to, and consistently increase in intensity near NNW striking normal faults in the backlimb (Figs. 6, 8 and 12) and NNE striking normal faults in the forelimb (Fig. 6). This joint set is similar to J1/J3 joints in the Aren group in three ways. First, they span a wide range of length/height sizes from cm to meter scale, and have similar sparry calcite fill. Second, both sets have a wide dispersion in dip, and have similar strike when grouped by structural position (Fig. 12 inset stereonet). Third, bed

strike-perpendicular joints in the Sant Corneli sequence consistently pre-date bed-oblique joint sets in the same way that J1/J3 joints in the Aren sequence pre-date J4/J5 joints, which are described in the following section. Because of the similarities with joints in the Aren Group, NNW striking joints in the backlimb and NNE striking joints in the forelimb are interpreted as J1/J3 joints.

### 3.2.5. Bed strike-oblique, calcite-filled joints with iron-oxidation (J4)

WNW striking joints are among the most systematic in the Aren group, with lengths greater than 5 m and spacing of 1–5 m (Figs. 9 and 14). WNW joints usually span the thicknesses of the sandy facies in the Aren (1–5 m thick) and are also commonly observed in the more resistant units of the finer grained, gray marls and deeper water facies, which suggests that they may span multiple stratigraphic units. Many WNW striking joints contain 1–3 mm of calcite fill, though one of the defining features of the WNW set is reddish iron oxidation and goethite mineral staining along and in the wall rock adjacent to such fractures. Wall rock staining spans the range from 5–10 cm haloes of light colored goethite mineralization (Fig. 15A and B) to lisegang banding in and around fractures (Fig. 15B and C). WNW striking joints consistently post-date both the NNE striking joints (J1/J3) and the NNW striking joints (J2) as indicated both by cross-cutting calcite fill and by joint termination relationships (Figs. 9 and 15). Some J4 joints are sinuous along their length.

Bed strike-oblique, locally calcite-filled joints in the forelimb of Sant Corneli anticline are correlated with WNW striking joints in the Aren group, although these joints rotate in strike as bed strike rotates around the anticline. These joints have outcrop trace

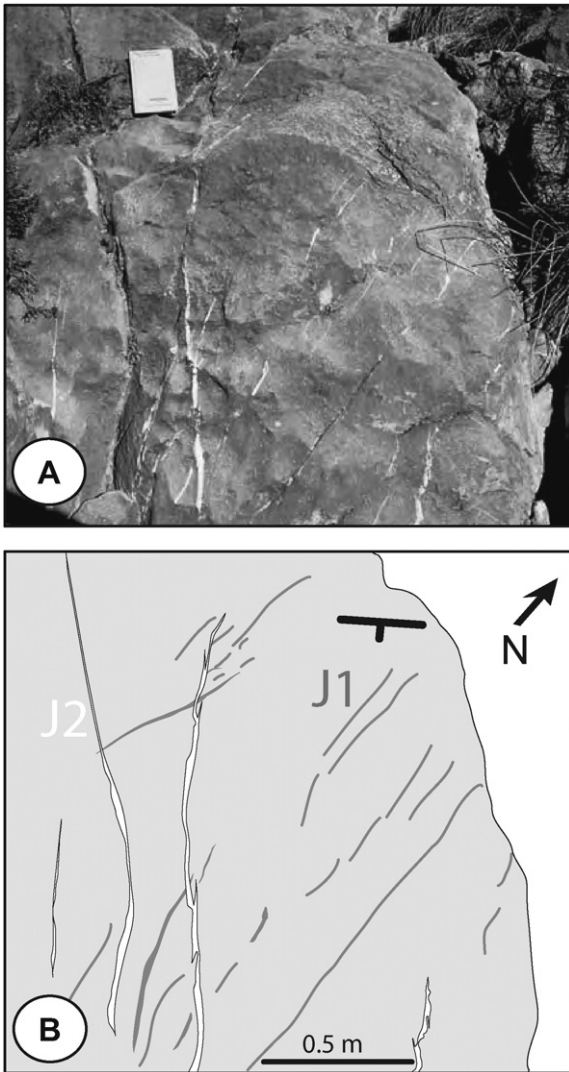


**Fig. 10.** Cross-cutting relationships of J1, J2, and J3 joints. Photo (A) and interpretive sketch (B) of J2 joints cross-cutting J1 joints in the Montesquiú sequence. At nearby outcrops, NNE striking joints (J3) that are similar to the J1 joints crosscut, and therefore post-date the J2 set, indicating subsets of NNE striking joints.

lengths of a meter or larger, with spacing greater than 0.7 m (Fig. 15). The trace in pavement outcrop of these joints is usually oriented less than  $45^\circ$  from bed strike in a clockwise sense, consistent with joints in the Aren group (Fig. 15). J4 joints have relatively thin ( $<2$  mm) to absent calcite fill and are locally mineralized with reddish iron oxidation and goethite mineral staining. In coarser wackestone/packstone lithologies, joints of this set are sinuous along their traces, with deviations from planarity on the order of a few millimeters to 2 cm ( $\sim 0.5$  cm “wavelength”). Cross-sectional exposures in the backlimb of the anticline indicate that some joints of this set have heights (perpendicular to bedding) of 10’s of meters. Bed strike-oblique joints of this set consistently crosscut bed strike-perpendicular joints of the J1/J3 set (Fig. 13).

### 3.2.6. Bed strike-oblique, calcite-filled joints with iron oxidation (J5)

E–NE striking calcite-filled joints of the Aren group are similar in character to the WNW striking (J4) joint set, with lengths greater than 5 m, local apertures of 1–2 mm, and similar iron oxidation and goethite mineralization (Fig. 15C and D). E–NE striking joints in the

Aren group are generally more poorly developed than WNW striking joints at the same localities, and are more commonly observed in the western end of the field area (Fig. 16). E–NE joints locally crosscut the WNW striking (J4) set, but the two sets may be coeval.

We distinguish a similar calcite-filled joint set in the Sant Corneli sequence, whose trace in pavement outcrops is oriented  $45^\circ$  or less counterclockwise from bed strike (Fig. 16). Joints of this set are similar in character to J4 joints in the Sant Corneli sequence and the Aren group in that they are locally sinuous, are locally calcite-filled, have associated iron oxidation, and post-date bed strike-perpendicular (J1/J3) joints (Fig. 13). Like J5 joints in the Aren group, this joint set is generally smaller in scale, has larger spacing, and is poorly developed relative to the J4 set in the Sant Corneli sequence, though the two sets intersect and share calcite fill in at least one sample site (Fig. 13).

## 4. Discussion and interpretations of fold–fracture evolution

While the tectono-stratigraphic evolution of the Sant Corneli–Bóixols anticlines has been well documented, no studies have extensively incorporated faulting and fracture timing relationships into their structural evolution. Here we discuss the relative timing of fracture sets with respect to the major structural and depositional episodes at Sant Corneli anticline.

### 4.1. NNE to NNW oriented normal faults

The predominance of west-dipping, NNW to NNE striking normal faults at Sant Corneli anticline has been recognized by various researchers. Such faulting is probably a combination of folding, uplift of Sant Corneli anticline, and gravitational collapse of the active margin into a westward deepening basin. Simó, et al. (1985) attribute faulting and slumps in the Vallcarga sequence to the onset of N–S compression and collapse of the outer margin towards the WNW, forming the Puimanyons Olistostrome (Fig. 7A). Guillaume et al. (2008) recognized an interruption of stratigraphic sequences in the Aren group, which they interpreted as a gravity driven collapse resulting from tilting and lateral propagation of Sant Corneli anticline at approximately late Cretaceous time based on the grade dating method (Gourinard, 1989). Banbury (2001) interpreted similarly oriented faults in the Boixols anticline as collapse features associated with outer arc extension along the axis of the Boixols anticline.

### 4.2. J1/J3 joints

Some J1/J3 joints in the Sant Corneli sequence, such as those on the backlimb of the anticline, have similar orientation to J2 joints in the forelimb and also some J5 joints on the fold nose (Figs. 12 and 16). However, J1/J3, J2, and J5 joints differ significantly in their character, specifically with respect to their dispersion in orientation, their size (length and height), their associated mineralization, and their spacing distribution. Unlike the J2 set, the J1/J3 joints are usually 1 m or less in length and height, have variable orientations, and are localized near faults. Conversely, J2 joints are usually a meter to a few meters in length and height, have almost no dispersion in orientation, and have very systematic spacing. Had we grouped such joints into a single set based on orientation, we would very likely have overlooked the relationship of such joints to local bed strike and to faulting.

NNE striking joints in the forelimb and NNW striking joints in the backlimb are oblique to the fold axis and to bed strike at Sant Corneli anticline, and are associated with similarly oriented faults that are sub-perpendicular to the fold axis (Figs. 6 and 12). This

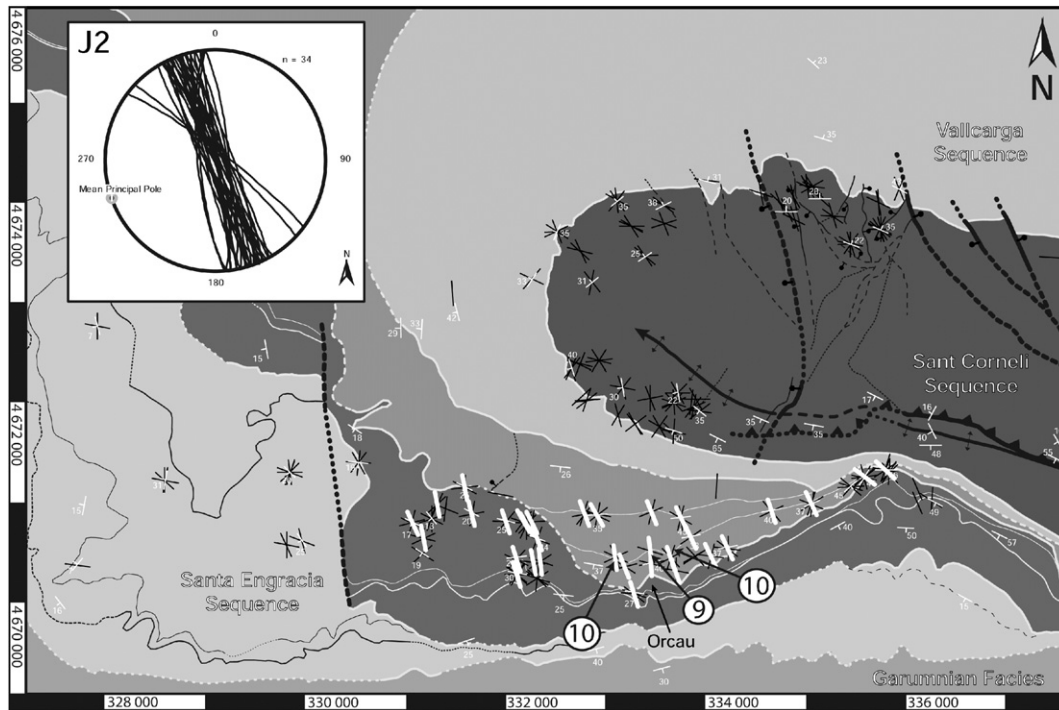


**Fig. 11.** Map of J2 joint strikes in the study area. White ticks indicate the strikes of J2 joints rotated to bed-horizontal. Black ticks indicate the strikes of all joint sets rotated to horizontal about the fold axis. Inset stereonet shows planes of J2 joints rotated to bed-horizontal. Circles with arrows indicate the numbers of figures showing J2 joints.

interpretation is supported by increasing intensity of J1 joints near these faults, the similarity in strike of the joints and faults, and that both the faults and the joints are mineralized with sparry calcite. While many of the axis sub-perpendicular faults and joints in the Sant Corneli sequence probably formed as a result of basin margin

collapse into a predominantly westward deepening basin during Puimanyons time (Simó, 1989), J1 joints in the Aren group must have formed after deposition and lithification of the Orcau-Vell sequence that they fracture (Fig. 17A). Therefore, we infer that normal faults occurred throughout the early to middle

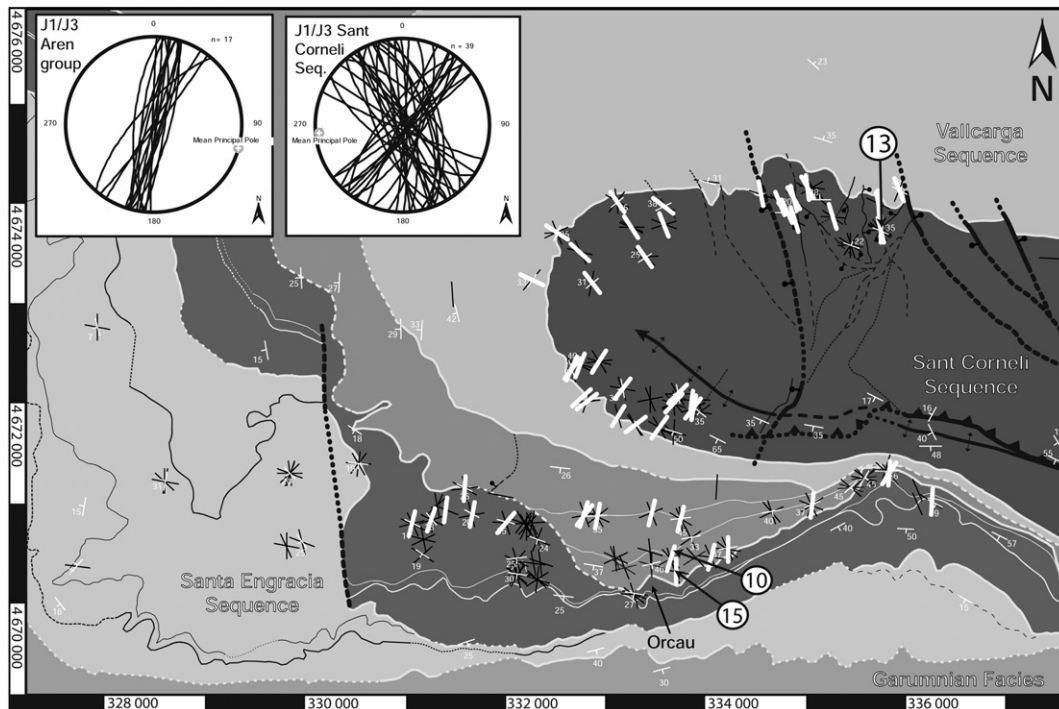


**Fig. 12.** Map of J1/J3 strikes in the study area. White ticks indicate the strikes of J1/J3 joints rotated to bed-horizontal. Black ticks indicate the strikes of all other joint sets rotated to horizontal about the fold axis. Inset stereonet shows planes of J1/J3 joints in the Aren Group and Sant Corneli sequence rotated to bed-horizontal. Circles with arrows indicate the numbers of figures showing J1/J3 joints.



**Fig. 13.** Photograph of an oblique cross section through bedding showing the relationship of J1/J3 to J4/J5 joints in the backlimb of the Sant Corneli Sequence. Inset sketch represents the area outlined by the dotted box in the image. The calcite fill of J4 and J5 are present along a previously filled J1/J3 joint. The inset sketch shows a J5 joint that terminates abruptly against the J1/J3 joint. A similar case is shown near the top of the image where a J4 joint curves into the J1/J3 joint. J4 and J5 joints appear to share calcite fill here.

development of Sant Corneli anticline and were reactivated during formation of the J1 and J3 subsets. We infer that J1 joints and normal faults formed in response to a combination of E–W stretching and basin margin collapse during the onset of fold propagation into the area.

The later J3 jointing may be a result of normal fault reactivation during intermediate stages of fold growth (Fig. 17B). Although earlier basin margin collapse could account for most of the

observed normal faulting, the collapse is unlikely to account for the sharp change in plunge of the fold axis of Sant Corneli anticline. The plunge of the anticline is approximately horizontal in the western end of the study area and abruptly steepens to nearly 25° where the Sant Corneli sequence subcrops below the Vallcarga sequence. This flexure along the axis of the fold could have reactivated existing normal faults and facilitated the development of J3 joints in the Aren group (Fig. 17B).

Without the timing constraints provided by syn-tectonic strata, the early joints (J1 and J3) could be interpreted to have formed during a pre-fold stage of regional E–W extension. If the stresses due to gravity sliding and normal faulting during early folding were greater than the flexural stresses within the folding layers, the orientation of the J1 and J3 joints would not exhibit folding even though folding had started. Although these joints formed during early folding, their orientation pattern provides no evidence of this early flexure (Savage et al., 2010).

4.3. J2 joints

We interpret J2 joints to have formed in response to layer parallel extension, possibly within the footwall of the interpreted gravity driven fault in the western end of the field area (Figs. 6 and 7B). Such faulting is expected to produce opening mode fractures parallel to the fault and localized within the units above the detachment, however, the orientation of the fault is not well constrained because the fault is not exposed at the surface and has been interpreted based on the offset of systems tracts. The systematic nature of such joints suggests that the extension was “regional” at the scale of the anticline, but is localized to the Aren group (Figs. 11 and 17A). The fact that we only observe the J2 set in the Aren group could be due to the difficulty in distinguishing J2 joints from similarly oriented J1/J3 and J5 joints in the underlying Sant Corneli sequence. We do not believe this is the case because

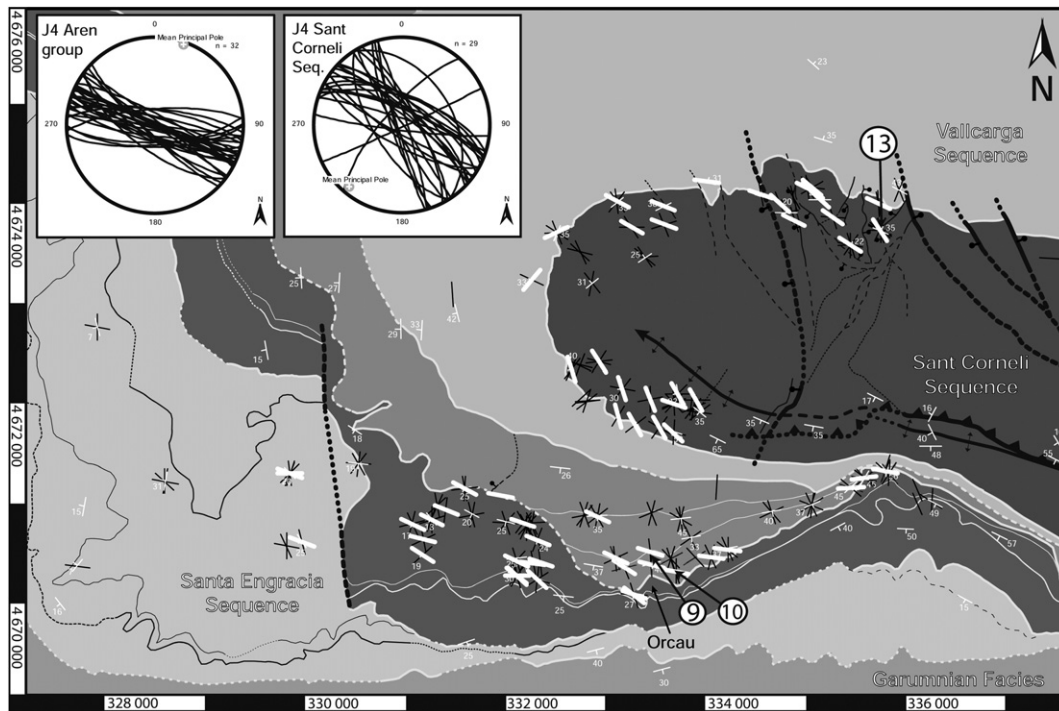


**Fig. 14.** Map of J4 strikes in the study area. White ticks indicate the strikes of J4 joints rotated to bed-horizontal. Black ticks indicate the strikes of all other joint sets rotated to horizontal about the fold axis. Inset stereonet shows planes of J4 joints in the Aren Group and Sant Corneli sequence rotated to bed-horizontal. Circles with arrows indicate the numbers of figures showing J4 joints.

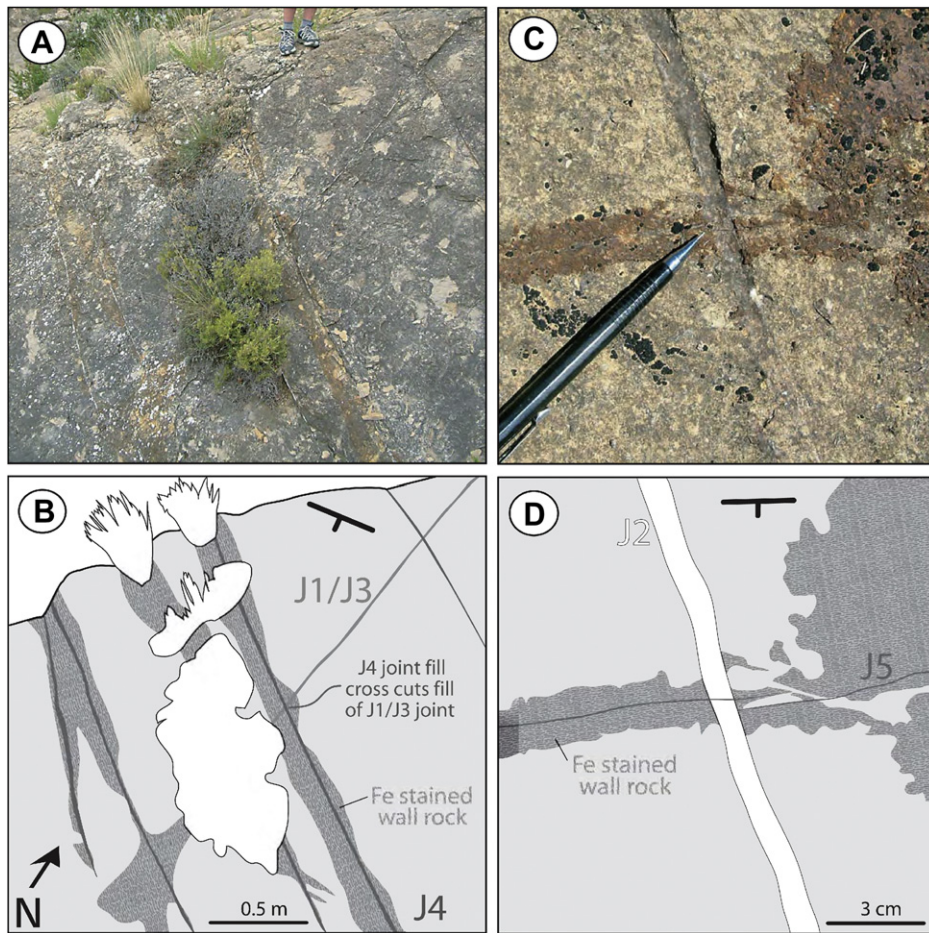


**Fig. 15.** Iron-oxidation along joints in the Aren sequence. Photo (A) and interpretive sketch (B) of bed-strike oblique (east) view of J4 joints on a pavement outcrop showing reddish goethite "haloes". Notice that J1/J3 joints immediately adjacent to the J4 joints have no associated oxidation. Photo (C) and interpretive sketch (D) of secondary liseegang banding associated with a J5 joint. The sub-millimeter thick calcite fill of the J5 joints crosscuts the calcite fill of a J2 joint indicating that the J5 joint crosscuts, and thus post-dates the J2 joint. Liseegang banding appears to be limited to a 2–3 cm thick zone adjacent to the J5 joints, with no liseegang banding associated with the J2 joints.

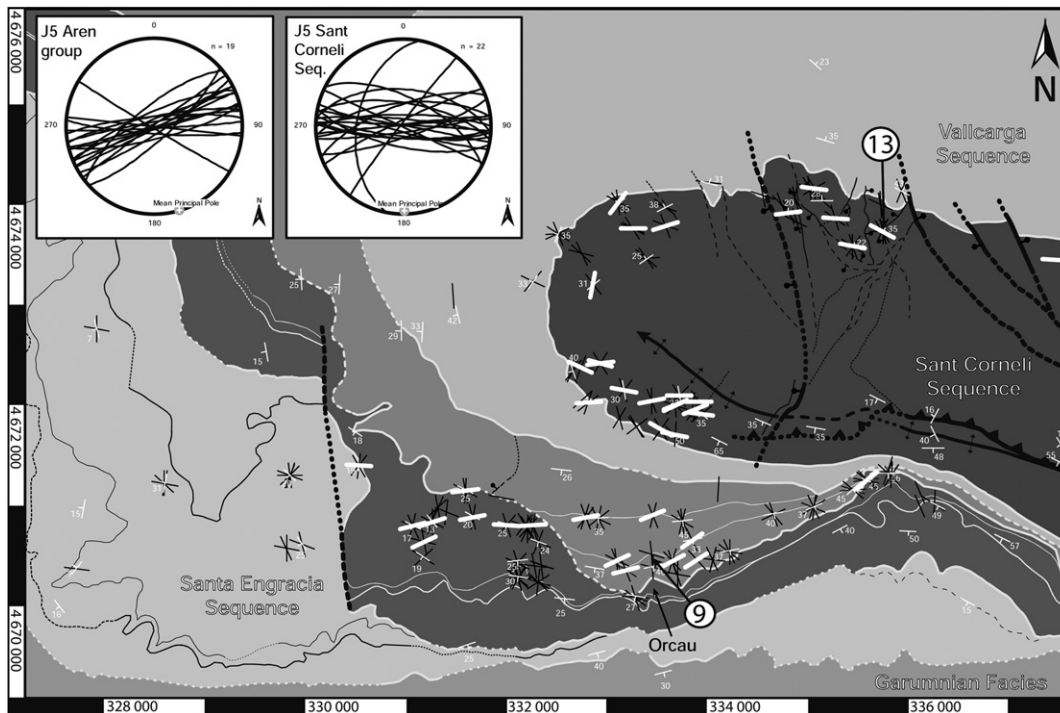


**Fig. 16.** Map of J5 strikes in the study area. White ticks indicate the strikes of J5 joints rotated to bed-horizontal. Black ticks indicate the strikes of all other joint sets rotated to horizontal about the fold axis. Inset stereonet shows planes of J5 joints in the Aren Group and Sant Corneli sequence rotated to bed-horizontal. Circles with arrows indicate the numbers of figures showing J5 joints.

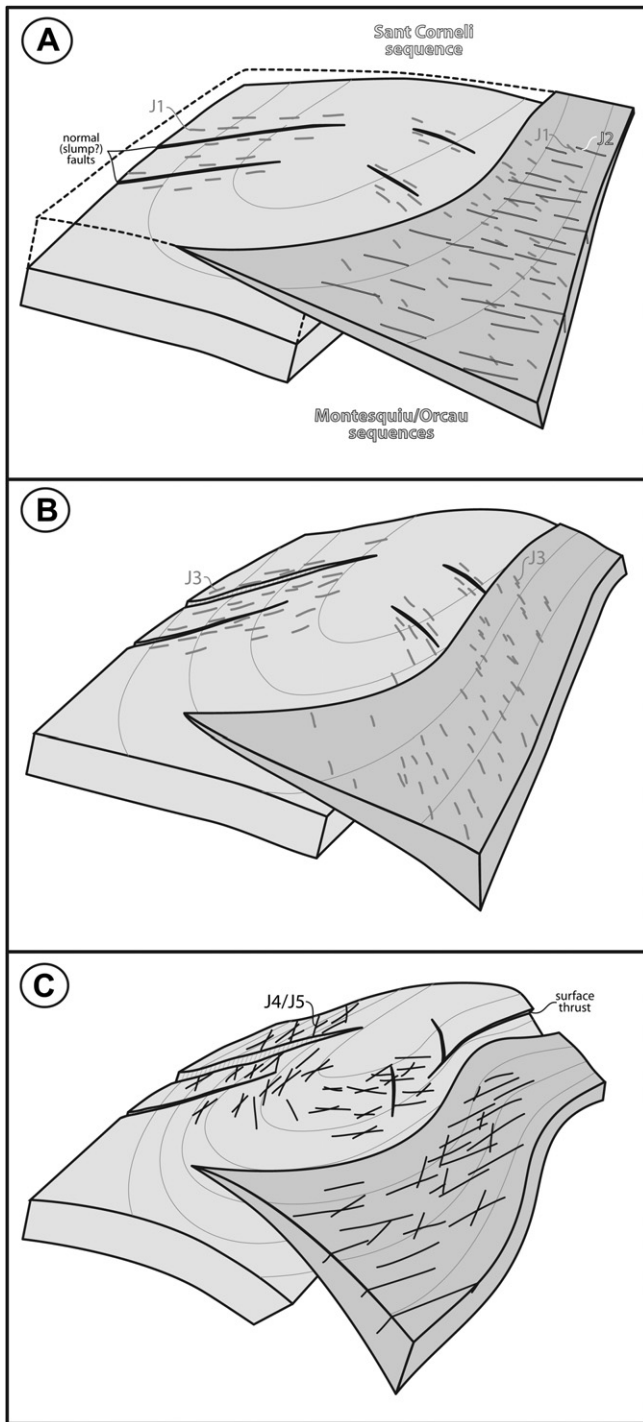


**Fig. 17.** Interpreted evolution of fracturing in Sant Corneli anticline. A) Montesquiú time through Orcau-Vell time (Fig. 7A–C): J1 jointing associated with early amplification of Sant Corneli anticline and may be associated with slumping. J1 joints within the Orcau-Vell sequence indicate that jointing occurred after the deposition of these units. J2 jointing may have occurred due to gravity faulting as interpreted by Guillaume et al. (2008) while the anticline was still at relatively low relief (Fig. 7F). B) Earliest Santa-Engracia time (Fig. 7D): J3 joints in the Montesquiú-Orcau sequences due to reactivation and further displacement on normal faults in the Sant Corneli sequence. C) Late Santa-Engracia to Eocene–Oligocene time (Fig. 7F): J4 and J5 joints are interpreted to have formed during the final stages of fold tightening in response to flexure of the anticline.

fractures in the Sant Corneli sequence with similar orientation to the J2 set do not have similar fracture mineralization, timing relationships with respect to one another, or size with respect to bedding.

#### 4.4. J4/J5 joints

J4/J5 joints are distinguished from older joint sets in the area by cross-cutting relationships, the close association of J4 and J5 joints with each other, and by distinct iron oxidation and goethite mineralization of the wall rock that is not observed in the J1, J2, and J3 sets (Figs. 13 and 15). The J4/J5 joints are interpreted to be a result of flexure of the anticline during the main stage of folding of Sant Corneli anticline as evidenced by their consistently changing orientation with respect to local bed strike. As bed strike changes around the fold, so too do the orientation of the J4/J5 joints (Fig. 18). The vertical distance between bedding and fracture data on Fig. 18 shows a consistent angle between bed azimuth and each fracture set azimuth, indicating that joint orientation changes consistently with bedding. Joints formed by regional stresses would be uniformly oriented and would form a horizontal line on Fig. 18. The oblique orientation of the J4 and J5 joints with respect to bed strike is consistent with plate bending models of non-cylindrical folds that predict joints oriented oblique to bed strike and the fold axis (Fischer and Wilkerson, 2000; Savage et al., 2010).

The obliquity of J4/J5 joints relative to the normal faults suggests that normal faulting had ceased by the time these joints formed. Stratigraphic evidence suggests that activity along the normal faults ceases by mid Paleocene time, or near the end of Santa Engracia sequence deposition (Déramond et al., 1993). Tilting of the Garumnian terrestrial deposits indicate that the Bóixols thrust was active during the latest Cretaceous and earliest Paleocene and that Sant Corneli anticline tightened during the Eocene–Oligocene time (Muñoz, 1992; Puigdefàbregas et al., 1992; Vergés, 1993). Therefore, J4/J5 jointing may have occurred as early as the last stage

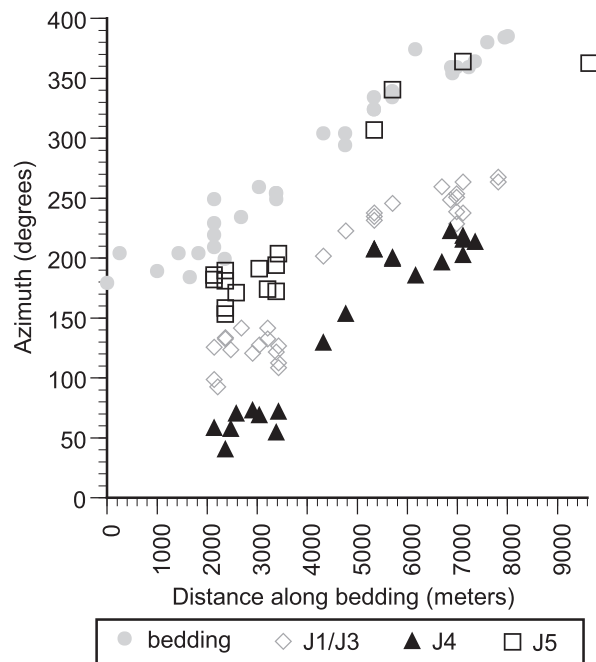


**Fig. 18.** Azimuth vs. traverse distance around the fold nose. Traverse shown in Fig. 6. The similar trend of the fracture sets and bed azimuths in the plot indicates that the fractures change orientation consistently with bedding. This pattern supports the interpretation that J4 and J5 joints are related to flexure of the anticline.

of Cretaceous–Paleocene, but more likely during the Eocene–Oligocene tightening of the anticline. Without such stratigraphic evidence, our study could not constrain the timing of joint formation relative to folding.

## 5. Conclusions and implications for studies of fold-related fracturing, faulting, and fluid flow

Our study is unique in that the correlation of different fracture sets to syn-tectonic sedimentation provides a direct link between fracturing events and the structural evolution of Sant Corneli anticline. The timing of J1, J2, and J3 joints relative to one another suggests that fold axis perpendicular normal faulting initiated relatively early in the folding process and occurred at least once more throughout the early growth of the anticline during at least Campanian and Maastrichtian time (Figs. 6 and 7D and 17A). We suggest that the pattern of normal faults is probably due to the influence of folding during basin margin collapse (Fig. 7A and 17A). J2 joints may have formed in response to gravity faulting interpreted by Guillaume et al. (2008) or simply as a result of normal gravitational sliding of the margin to the west (Fig. 17A). Late-stage joints (J4/J5, Figs. 13–17) are generally closer to bed strike and are commonly associated with goethite and iron oxidation, which distinguishes them from earlier fracture sets. We interpret J4 and J5 joints to be a result of flexure of the anticline during the main stage of folding based on their consistent orientation with respect to bedding.

The results of this study demonstrate the necessity of distinguishing fracture sets based on a variety of characteristics and not solely on their present orientation. Plate bending models and mechanical models for folding predict spatially heterogeneous stress fields around non-cylindrical structures where local bed orientation may change rapidly over short distances (Stearns, 1967; Stearns and Friedman, 1972; Szilard, 1974; Maerten, 1999; Fischer and Wilkerson, 2000; Hennings et al., 2000; Moretti et al., 2006). Thus, the fracture sets associated with non-cylindrical folding may correlate better with local bed strike than with a fixed structural orientation (Figs. 17 and 18). Fracture, mode, mineralization, and size can be used in conjunction with orientation to group fracture sets that may have formed in response to spatially heterogeneous stress fields. Additionally, sequential restoration of syn-tectonic strata can constrain transitional fold shapes and the stress/strain history of fault-related folds. Where syn-tectonic strata are absent, forward modeling and interpolation between deformed and restored fold shapes may be used to constrain transitional fold shapes.

Many of the fracture sets and faults at Sant Corneli anticline are mineralized with calcite and other cements that indicate the importance of such structures for fluid flow in the anticline. The distinct difference in cementation between J1, J2, J3 joints (calcite only) and J4/J5 joints (calcite with hematite/goethite) may indicate changing fluid flow regimes during folding. Furthermore, cross-cutting relationships of different phases of calcite fill (e.g. Figs. 10, 13 and 15) suggest that healing of joint sets can be relatively common. Geochemical analyses and fluid inclusion analyses of calcite-filled fractures and faults could further constrain the timing and boundary conditions (pressure/temperature) under which many of the fracturing events occurred.

## Acknowledgements

This research was made possible by funding from the University of Massachusetts (Faculty Research Grant), the American Association of Petroleum Geologists, the Geological Society of America, Sigma Xi, and Midland Valley Exploration Ltd. We would also like to acknowledge Mike Apfelbaum, Scott Marshall, Gemma Labraña, and the Institute of Earth Sciences 'Jaume Almera' for support of

field work. We would also like to thank Nicolas Bellahsen, Scott Wilkins and Bill Dunne for very constructive comments that improved this manuscript.

## References

- Arbués, P., Pi, E., Berástegui, X., 1996. Relaciones entre la evolución sedimentaria del Grupo de Arén y el Cabalgamiento de Boixols (Campaniense terminal-Maastrichtiense del Pirineo Meridional-Central). *Geogaceta* 20, 446–449.
- Ardévol, L., Klimowitz, J., Malagón, J., Nagtegaal, P.J.C., 2000. Depositional sequence response to foreland deformation in the upper cretaceous of the southern Pyrenees, Spain. *American Association of Petroleum Geologists Bulletin* 84 (4), 566–587.
- Banbury, N., 2001. The role of hanging-wall structure in thrust systems, examples from the South Pyrenean foreland fold and thrust belt, northern Spain, Unpublished Master of Research thesis, University of Edinburgh.
- Bellahsen, N., 2006. The role of fractures in the structural interpretation of sheep mountain anticline, Wyoming. *Journal of Structural Geology* 28 (5), 850–867.
- Bellahsen, N., Fiore, P.E., Pollard, D.D., 2006. From spatial variation of fracture patterns to fold kinematics; a geomechanical approach. *Geophysical Research Letters* 33 (2).
- Berástegui, X., García-Senz, J.M., Losantos, M., 1990. Tecto-sedimentary evolution of the organya extensional basin (central south Pyrenean unit, Spain) during the lower cretaceous. *Bulletin de la Societe Geologique de France* 8 (2), 250–253.
- Bergbauer, S., Pollard, D.D., 2004. A new conceptual fold-fracture model including pre-folding joints, based on the emigrant gap anticline, Wyoming. *Geological Society of America Bulletin* 116 (3–4), 294–307.
- Bernal, A., Hardy, S., 2002. Syn-tectonic sedimentation associated with three-dimensional fault-bend fold structures; a numerical approach. *Journal of Structural Geology* 24 (4), 609–635.
- Bond, R.M.G., McClay, K.R., 1995. Inversion of a lower cretaceous extensional basin, south central Pyrenees, Spain. In: *Geological Society Special Publications*, 88, pp. 415–431. London.
- Cooper, M., 1992. The Analysis of Fracture Systems in surface thrust structures from the foothills of the Canadian Rockies. In: McClay, K.R. (Ed.), *Thrust Tectonics*. Chapman & Hall, London, United Kingdom, pp. 391–405.
- Déramond, J.D., Souquet, P., Fondcave-Wallez, M.J., Specht, M., 1993. Relationships between thrust tectonics and sequence stratigraphy surfaces in foredeeps: model and examples from the Pyrenees (Cretaceous-Eocene, France, Spain). In: Williams, G.D., Dobb, A. (Eds.), *Tectonics and Seismic Sequence Stratigraphy*. Geological Society Special Publication, 71, pp. 193–219. London.
- Engelder, T., Gross, M.R., Pinkerton, P., 1997. Joint development in clastic rocks of the Elk basin anticline, Montana-Wyoming: an analysis of fracture spacing versus bed thickness in a basement involved Laramide structure. In: 1997 *Fractured Reservoir Field Guidebook*. Rocky Mountain Association of Geologists, pp. 1–18.
- Erslev, E.A., 1991. Trishear fault-propagation folding. *Geology* 19, 617–620.
- Fischer, M.P., Wilkerson, M.S., 2000. Predicting the orientation of joints from fold shape; results of pseudo-three-dimensional modeling and curvature analysis. *Geology* 28 (1), 15–18.
- Ford, M., Williams, E.A., Artoni, A., Vergés, J., Hardy, S., 1997. Progressive evolution of a fault-related fold pair from growth strata geometries, Sant Llorenç de Morunys, SE Pyrenees. *Journal of Structural Geology* 19 (3–4), 413–441.
- García-Senz, J., 2002. Cuencas extensivas del Cretácico inferior en los Pirineos Centrales, formación y subsecuente inversión, Unpublished Ph.D. thesis, University of Barcelona, Spain.
- Garrido-Megías, A., Ríos Aragües, L.M., 1972. Síntesis geológica del Secundario y Terciario entre los ríos Cinca y Segre (Pirineo Central de la vertiente sur pirenaica, provincias de Huesca y Lérida). *Boletín Geológico y Minero* 83, 1–47.
- Gourinard, Y., 1989. Grade-dation et modalités de l'évolution. (Grade dating and modes of evolution). *Bulletin Centres Recherche Exploration-Production Elf-Aquitaine* 13 (2), 417–424.
- Griffiths, P., Jones, S., Salter, N., Schaefer, F., Osfield, R., Reiser, H., 2002. A new technique for 3-D flexural-slip restoration. *Journal of Structural Geology* 24 (4), 773–782.
- Grout, M.A., Verbeek, E.R., 1998. Tectonic and paleostress significance of the regional joint network of the central paradox basin, Utah and Colorado. In: Friedman, J.D., Huffman Jr., A.C. (Eds.), *Laccolith Complexes of Southeastern Utah: Tectonic Control and Time of Emplacement—Workshop Proceedings*. U.S. Geological Survey Bulletin, pp. 151–166. 2158.
- Guillaume, B., Dhont, D., Brusset, S., 2008. Three-dimensional geologic imaging and tectonic control on stratigraphic architecture: upper cretaceous of the tremp Basin (south-central Pyrenees, Spain). *American Association of Petroleum Geologists Bulletin* 92 (2), 249–269.
- Hanks, C.L., Lorenz, J., Teufel, L., Krumhardt, A., 1997. Lithologic and structural controls on natural fracture distribution and behavior within the Lisburne group, northeastern Brooks range and north slope subsurface, Alaska. *American Association of Petroleum Geologists Bulletin* 81 (10), 1700–1720.
- Hennings, P.H., Olson, J.E., Thompson, L.B., 2000. Combining outcrop data and three-dimensional structural models to characterize fractured reservoirs; an example from Wyoming. *American Association of Petroleum Geologists Bulletin* 84 (6), 830–849.

- Johnson, K.M., Johnson, A.M., 2002. Mechanical models of trishear-like folds. *Journal of Structural Geology* 24 (2), 277–287.
- Lanaja, J.M., Querol, R., Navarro, A., 1987. Contribución de la exploración petrolífera al conocimiento de la geología de España. Instituto Geológico y Minero de España.
- Maerten, F., Maerten, L., 2006. Chronologic modeling of faulted and fractured reservoirs using a geomechanically based restoration: technique and industry applications. *American Association of Petroleum Geologists Bulletin* 90 (8), 1201–1226.
- Maerten, L., 1999. Mechanical interaction of intersecting normal faults; theory, field examples and applications. Unpublished Ph.D. thesis, Stanford University.
- McGrath, A.G., Davison, I., 1995. Damage zone geometry around fault tips. *Journal of Structural Geology* 17, 1011–1024.
- Mellere, D., 1993. Thrust generated, back-fill stacking of alluvial fan sequences, south-central Pyrenees, Spain (La Poblá de Segur Conglomerates). *International Association of Sedimentologists, Special Publication* 20, 259–276.
- Moretti, I., Lepage, F., Guiton, M., 2006. KINE3D: a new 3D restoration method based on a mixed approach linking geometry and geomechanics. *Oil & Gas Science and Technology* 61 (2), 277–289.
- Muñoz, J.A., 1992. Evolution of a continental collision belt. ECORS – Pyrenees crustal Balanced cross-section. In: McClay, K.R. (Ed.), *Thrust Tectonics*. Chapman & Hall, London, pp. 235–246.
- Nagtegaal, P.J.C., Van Vliet, A., Brouwer, J., 1983. Sytectonic coastal offlap and concurrent turbidite deposition: the upper Cretaceous Aren sandstone in the south-central Pyrenees, Spain. *Sedimentary Geology* 34, 185–218.
- Nigro, F., Renda, P., 2004. Growth pattern of underlithified strata during thrust-related folding. *Journal of Structural Geology* 26 (10), 1913–1930.
- Novoa, E., Suppe, J., Shaw, J.H., 2000. Inclined-shear restoration of growth folds. *American Association of Petroleum Geologists Bulletin* 84 (6), 787.
- Pavlis, T.L., Bruhn, R.L., 1988. Stress history during propagation of a lateral fold-tip and implications for the mechanics of fold-thrust belts. *Tectonophysics* 145, 1–2.
- Poblet, J., McClay, K., 1996. Geometry and kinematics of single-layer detachment folds. *American Association of Petroleum Geologists Bulletin* 80, 1085–1109.
- Poblet, J., Muñoz, J.A., Travé, A., Serra-Kiel, J., 1998. Quantifying the kinematics of detachment folds using three-dimensional geometry; application to the median anticline (Pyrenees, Spain). *Geological Society of America Bulletin* 110 (1), 111–125.
- Pollard, D.D., Aydin, A., 1988. Progress in understanding jointing over the past century. *Geological Society of America Bulletin* 100, 1181–1204.
- Puigdefàbregas, C., Muñoz, J.A., Vergés, J., 1992. Thrusting and foreland basin evolution in the southern Pyrenees. In: McClay, K. (Ed.), *Thrust Tectonics*. Chapman & Hall, London, pp. 247–254.
- Puigdefàbregas, C., Souquet, P., 1986. Tecto-sedimentary cycles and depositional sequences of the mesozoic and tertiary from the Pyrenees. *Tectonophysics* 129, 173–203.
- Roest, W.R., Srivastava, S.P., 1991. Kinematics of the plate boundaries between Eurasia, Iberia, and Africa in the north Atlantic from the late cretaceous to the present. *Geology* 19, 613–616.
- Rouby, D., Xiao, H., Suppe, J., 2000. 3-D restoration of complexly folded and faulted surfaces using multiple unfolding mechanisms. *American Association of Petroleum Geologists Bulletin* 84 (6), 805–829.
- Rudnicki, J.W., Wu, M., 1995. Mechanics of dip-slip faulting in an elastic half-space. *Journal of Geophysical Research* 100 (B11), 22173–22186.
- Salvini, F., Storti, F., 2002a. Three-dimensional architecture of growth strata associated to fault-bend, fault-propagation, and decollement anticlines in non-erosional environments. *Sedimentary Geology* 146, 1–2. January.
- Salvini, F., Storti, F., 2002b. Three-dimensional architecture of growth strata associated to fault-bend, fault-propagation, and decollement anticlines in non-erosional environments. *Sedimentary Geology* 146, 1–2.
- Savage, H.M., Cooke, M.L., 2004. The effect of non-parallel thrust fault interaction on fold patterns. *Journal of Structural Geology* 26 (5), 905–917.
- Savage, H.M., Shackleton, J.R., Cooke, M.L., Riedel, J.J., 2010. Insights into fold growth using fold-related joint patterns and mechanical stratigraphy. *Journal of Structural Geology* 32 (10), 1466–1475.
- Shackleton, J.R., 2003. The Relationship between Fracturing, Asymmetric Folding, and Normal Faulting in Lisburne Group Carbonates: west Porcupine Lake Valley, Northeastern Brooks Range, Alaska, Unpublished Masters thesis, University of Alaska.
- Simó, J.A., 1985. Secuencias Depositionales del Cretaco superior de la Unidad del Montsec Pirineo Central, Unpublished Ph.D. thesis, University of Barcelona.
- Simó, J.A., 1989. Upper cretaceous platform-to-basin depositional-sequence development, tremp basin, south-central Pyrenees, Spain. In: Crevello, P.D., Wilson, J.L., Sarg, J.F., Read, J.F. (Eds.), *Controls on Carbonate Platforms and Basin Development*. SEPM Special Publication, 44, pp. 365–378.
- Simó, J.A., Puigdefàbregas, C., Gili, E., 1985. Transition from shelf to basin on an active slope, upper cretaceous tremp area, southern Pyrenees. In: Mila, M.D., Rosell, J. (Eds.), *International Association of Sedimentologists, Sixth European Regional Meeting: Excursion Guidebook*, pp. 63–108.
- Specht, M., Déramond, J., Souquet, P., 1991. Relations tectonique-sédimentation dans les bassins d'avant-pays; utilisation des surfaces stratigraphiques isochrones comme marqueurs de la déformation. *Bulletin de la Société Géologique de France* 162 (3), 553–562.
- Stearns, D.W., 1967. Certain aspects of fractures in naturally deformed rocks. In: Riecker, R.E. (Ed.), *NSF Advanced Science Seminar in Rock Mechanics*, pp. 97–118. Air Force Cambridge Research Lab Report, Bedford, MA.
- Stearns, D.W., Friedman, M., 1972. Reservoirs in fractured rock. *Memoir American Association of Petroleum Geologists* 16 (10), 82–106.
- Suppe, J., 1983. Geometry and kinematics of fault-bend folding. *American Journal of Science* 283, 684–721.
- Suppe, J., Medwedeff, D.A., 1990. Geometry and kinematics of fault-propagation folding. *Ecologiae Helvetiae* 83, 409–454.
- Szilard, R., 1974. *Theory and Analysis of Plates: classical and Numerical Methods*. Prentice Hall.
- Thibert, B., Gratier, J.P., Morvan, J.M., 2005. A direct method for modeling and unfolding developable surfaces and its application to the ventura basin, California. *Journal of Structural Geology* 27 (2), 303–316.
- Van Hoorn, B., 1970. Sedimentology and paleogeography of an upper cretaceous turbidite basin in the south-central Pyrenees, Spain. *Leidse Geologische Mededelingen* 45, 73–154.
- Vergés, J., 1993. Estudi geologic del vessant Sud del Pirineu Oriental i Central: Evolucio en 3D. Unpublished Ph.D. thesis, University of Barcelona.
- Vergés, J., Burbank, D.W., Meigs, A., 1996. Unfolding; an inverse approach to fold kinematics. *Geology* 24 (2), 175.